UC San Diego

UC San Diego Previously Published Works

Title

Hydrogen-deuterium exchange mass spectrometry reveals folding and allostery in protein-protein interactions

Permalink

https://escholarship.org/uc/item/6qg7s5zn

Authors

Ramirez-Sarmiento, Cesar A
Komives, Elizabeth A

Publication Date

2018-07-01

DOI

10.1016/j.ymeth.2018.04.001

Peer reviewed

eScholarship.org Powered by the California Digital Library
University of California

Author Manuscript

Author Manuscript

Author Manuscript

Author Manuscript

HHS Public Access

Author manuscript

Methods. Author manuscript; available in PMC 2019 July 15.

Published in final edited form as:

Methods. 2018 July 15; 144: 43–52. doi:10.1016/j.ymeth.2018.04.001.

Hydrogen-Deuterium Exchange Mass Spectrometry Reveals Folding and Allostery in Protein-Protein Interactions

Cesar A. Ramirez-Sarmiento[1] and **Elizabeth A. Komives**[2,*]

[1]Institute for Biological and Medical Engineering, Schools of Engineering, Medicine and Biological Sciences, Pontificia Universidad Catolica de Chile, Av. Vicuña Mackenna 4860, Santiago 7820436, Chile

[2]Department of Chemistry and Biochemistry, University of California, San Diego, 9500 Gilman Drive, La Jolla, CA 92092-0378

Abstract

Hydrogen-deuterium exchange mass spectrometry (HDXMS) has emerged as a powerful approach for revealing folding and allostery in protein-protein interactions. The advent of higher resolution mass spectrometers combined with ion mobility separation and ultra-high liquid chromatographic separations have allowed the complete coverage of large protein sequences and multi-protein complexes. Liquid-handling robots have improved the reproducibility and accurate temperature control of the sample preparation. Many researchers are also appreciating the power of combining biophysical approaches such as stopped-flow fluorescence, single molecule FRET, and molecular dynamics simulations with HDXMS. In this review, we focus on studies that have revealed (re)folding of proteins as well as on long-distance allosteric changes upon interaction.

Graphical abstract

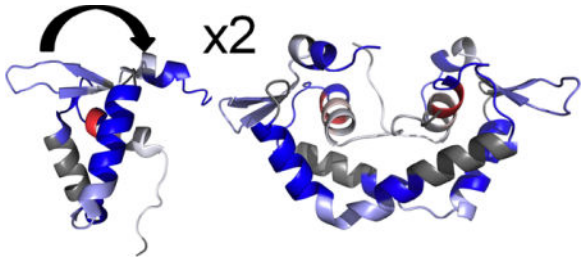

1. Introduction

The biophysical characterization of protein folding and protein-protein interactions has been largely carried out through the use of optical spectroscopy approaches, in which the optical

*Corresponding author: Elizabeth A. Komives, Department of Chemistry and Biochemistry, University of California, San Diego, 9500 Gilman Drive, La Jolla, CA 92092-0378, Ph: (858) 534-3058, ekomives@ucsd.edu.

Publisher's Disclaimer: This is a PDF file of an unedited manuscript that has been accepted for publication. As a service to our customers we are providing this early version of the manuscript. The manuscript will undergo copyediting, typesetting, and review of the resulting proof before it is published in its final citable form. Please note that during the production process errors may be discovered which could affect the content, and all legal disclaimers that apply to the journal pertain.

Author Manuscript Author Manuscript Author Manuscript Author Manuscript

signal is sensitive to the breaking or forming of protein interactions. An example of such an approach is far- and near-UV circular dichroism, which allows for monitoring of the folding and/or binding-dependent changes in secondary and tertiary structure within a protein sample respectively [1], but the optical response is the result of a global change in dichroic signal and rarely allow for the localization where these changes are occurring. Tryptophan fluorescence is a popular approach for studying the changes in protein folding upon interaction, but in this case the tryptophan generally only probes a local conformational change [2]. Other methods that use fluorescence require the introduction of a fluorescent probe possibly creating artifacts due to subtle changes in the structure of the folded state [3]. Fluorescence anisotropy is a popular approach for the assessment of protein-protein complex formation [4], but this again is a global approach and does not yield information about where or how the interaction occurs within the protein.

Amide hydrogen/deuterium exchange was originally pioneered as an indicator of protein folding [5]. In 1998, we demonstrated that if the rapidly exchanging surface amides could be detected by mass spectrometry, the solvent accessibility decrease upon interface formation could be measured allowing localization of the interface [6]. Surface amides exchange within a time period so short that they have already exchanged by the first measurable timepoint in a classical NMR H/D exchange experiment (~10 min). Therefore hydrogen-deuterium exchange mass spectrometry (HDXMS) is the method of choice for measuring changes in exchange on protein surfaces. Surface amides that are not hydrogen-bonded exchange much more slowly than would be expected for a completely unstructured peptide [7] indicating the solvent accessibility definitely plays a role in the broad range of exchange rates of surface amides. We and others have found that measurement of exchange times of 0-5 min best highlights differences due to binding solvent accessibility changes at protein surfaces [8]. One must also consider the binding affinity of the complex, which generally gives some idea of the dissociation rate and consequently how long the complex remains bound under the experimental conditions. For weakly bound complexes (K_D above 10 nM), an excess of ligand should be used to robustly detect the interface protection [8]. If crystal structures are available, it is possible to estimate the number of amides that will be protected from exchange simply by computationally assessing the difference in solvent accessibility between the free proteins and the bound complex. Often only a few amides are expected to be sequestered from exchange at the interface [9]. In addition, many proteins contain disordered regions that become more folded upon engagement of their binding partner. These situations reveal themselves by a much larger number of amides showing decreased exchange than cannot be accounted for by a simple difference in solvent accessibility computed from the structure of the individual proteins from the complex [10]. With this background in mind, we would like to highlight a few protein-protein interactions where changes in folding and or interaction were observed. We have chosen examples where the interpretation of the data critically relied on other observables, either circular dichroism, fluorescence, or both.

Author Manuscript Author Manuscript Author Manuscript Author Manuscript

2. Results and Discussion

2.1 Proteins that fold or re-fold upon interaction with a binding partner

The majority of proteins fold into oligomers. Indeed, 81% of the *E. coli* proteome [11], and even 26% of the simplest bacteria, *Mycoplasma pneumoniae* proteome is constituted by oligomers [12]. Often the formation of the oligomer is coupled to the folding of the monomeric unit. In more complex eukaryotic organisms, where dynamic protein-protein interactions are fundamental for enabling a diversification of protein functions in space and time [13], an extensive amount of evidence has demonstrated strong coupling between folding and binding. For most oligomers whose monomers are larger than 100 residues, subunits dissociate into folding intermediates comprising single or multiple polypeptide chains [14]. For smaller proteins, monomers are more likely to remain folded after dissociation if the surface area buried upon dimerization is small and the monomer is compact [14].

Although interactions between monomers are as essential as interactions within monomers for inducing subunit folding, a remaining question is which parts of a given protein remain folded upon dissociation, i.e. the extensibility of the coupling between folding and binding. HDXMS allows for localization of the changes occurring within a protein structure upon association/dissociation [6, 15]. In this experiment, a comparative analysis is usually performed between a sample of the native protein complex and a second sample characterized by: i) the addition of a chemical or temperature perturbation that induces dissociation [16]; ii) a mutant variant that shifts the equilibrium towards dissociation of the protein complex [17]; or iii) the absence of one of the binding partners, as in the case of heterocomplexes [10].

2.1.1 Unfolding and refolding in Serine Protease INhibitors, SERPINS—Serpins natively fold to an active conformation which contains a large unfolded, surface-exposed reactive center loop (RCL). Protease cleavage of the RCL in the serpin results in covalent attachment of the protease to the N-terminal half of the RCL followed by a 70 Å translocation of the protease to the opposite pole of the serpin and insertion of the protease-linked part of the RCL into the central β-sheet A of the serpin. This translocation distorts the active site of the entrapped protease and inhibits its ability to release itself from the inhibitory complex with the serpin [18]. SERPINS are also known to enter a latent conformation and to aggregate in diseases known as serpinopathies [19].

The characterization of the slow unfolding and refolding of the RCL in plasminogen activator inhibitor 1 (PAI-I) required careful exploration of the temperature dependence of the amide exchange [20] and ultimately the mechanism was determined by integration of MD simulations and HDXMS [21]. Alpha-1-antitrypsin was the first SERPIN to be studied by HDXMS [22]. A combination of temperature studies and protein kinetics have revealed how this SERPIN folds avoiding aggregation [23].

2.1.2 Dimerization of Phosphofructokinase-2—Phosphofructokinase-2 (Pfk-2), a homodimeric enzyme from *E. coli*, is one of the largest proteins that exhibits unfolding upon both cooling above the freezing point of water and heating [24]. The protein-protein

Author Manuscript Author Manuscript Author Manuscript Author Manuscript

interface of this homodimer corresponds to a small domain that emerges as a topological discontinuity [25] on the polypeptide chain of a larger domain that contains the ligand-binding sites [26], i.e. there are 4 chain crossings between these domains. Such increase in complexity of the chain topology is not unique to Pfk-2 and is known to enable cooperative folding between domains [27]. Moreover, both chemical [28] and temperature [24] perturbations lead to a compact monomeric intermediate with remaining secondary structure, as determined by circular dichroism, intrinsic fluorescence of a single tryptophan located within the protein-protein interface and size exclusion chromatography. However, given the reentrant connectivity of the polypeptide chain, a remaining question was whether the dissociation-induced unfolding was occurring throughout the protein structure or if there were localized regions that were unaffected by the disassembly of the complex, such as the C-terminal domain of the large domain of Pfk-2 that is not interrupted by the insertion of the small domain [26]. To solve this conundrum, HDXMS was employed to decipher the extent of coupling between folding and binding for the Pfk-2 homodimer by taking advantage of the cold denaturation that this protein experiences above the freezing point of water. A sample of Pfk-2 at 25° C was compared to another sample of Pfk-2 incubated for 24 h at 4° C by measuring the plateau of maximum deuterium exchange after several minutes of incubation [16]. We used MALDI-TOF MS to measure HDXMS and were able to analyze the data from eight peptides distributed across the whole protein structure and representing coverage of 27% of the Pfk-2 sequence. For all regions, the extent of exchange was higher (average deuterium exchange ~72%) than in the native dimer at 25° C (average maximum exchange ~23%), but still far from the ~100% expected for a fully unfolded protein. Moreover, the kinetics of the increase in exchange over time at 4°C were quantified by taking time points hourly during the slow cold-denaturation process, followed by HDXMS analysis for each time point. Given that one of the peptides covered the protein-protein interaction surface, the first step was to compare the kinetics of cold-denaturation obtained by HDXMS with those coming from a fluorescence intensity decay of a single tryptophan (W88) located at the subunit interface. The fluorescence kinetics of this single tryptophan fully matched the rates obtained from HDXMS analysis (1.3×10^{-4} s^{-1} by tryptophan fluorescence; 1.0×10^{-4} s^{-1} for change in deuteration over time for residues 104 – 113 as measured by HDXMS). Remarkably, rates of increasing exchange for every region analyzed via HDXMS were, on average, 1.0×10^{-4} s^{-1}, thus suggesting that cold-denaturation led to a concerted partial unfolding of Pfk-2 throughout the whole protein structure. The extent of exchange of the cold-denatured ensemble after 24 h of incubation in the cold was also similar to that of the chemically induced monomeric intermediate formed upon incubation of Pfk-2 at 25 °C in the presence of 0.85 M GndHCl. Later experiments on a qTOF mass spectrometer allowed for 100% sequence coverage and confirmed that the whole enzyme was swollen upon cold-denaturation.

Although the aforementioned experiments were revealing, both temperature and chemically induced dissociation/unfolding are phenomena that act globally on a given protein, whereas mutations that destabilize the protein-protein interface only shift the equilibrium towards the isolated subunit. Therefore, a second line of evidence was generated based on the generation of a mutant of Pfk-2 (L93A) that destabilized the protein-protein interaction [17]. This mutant, which was confirmed by size exclusion chromatography, SAXS, analytical

Author Manuscript Author Manuscript Author Manuscript Author Manuscript

ultracentrifugation and enzyme kinetics to correspond to an inactive monomer at protein concentrations below 30 μM and to be more compact than the cold-denatured ensemble [16], also formed a dimer upon addition of the enzyme's natural substrate, fructose-6-phosphate. HDXMS measurements on a Synapt G2Si qTOF mass spectrometer combined with ultra-high liquid chromatographic separations and automated liquid handling were performed for the native dimer and for the L93A mutant in the absence or presence of fructose-6-phosphate, covering 99% of the full protein sequence. The results revealed that, in contrast to the observations made from the cold-denaturation experiments, the deuterium uptake into the C-terminus of the L93A mutant (residues 240–309) was not much different from that of the wild-type enzyme and the substrate-induced dimer (Figure 1). Interestingly, this region constitutes a module within the large domain of Pfk-2 that is not interrupted by the topological discontinuity of the polypeptide chain and which contains most of the residues that interact with ATP [29]. Chemical unfolding experiments of the L93A mutant followed by circular dichroism showed that this variant unfolded noncooperatively upon increasing concentrations of denaturant. Altogether, these results demonstrated that the folding unit of Pfk-2 corresponds to the bimolecular domain constituted by the protein-protein interaction established between the small domains from two monomers of Pfk-2 and by the module of the large domain that was topologically wired to the dimerization domain through the polypeptide chain connectivity (Figure 1). This example also illustrates beautifully how HDXMS aids in bridging the gap between classic biophysical experiments and a molecular picture of the folding-upon-binding phenomenon.

2.1.3 FoxP1—Most of the structural changes discussed above correspond to large folding/unfolding transitions upon the establishment of protein-protein interactions. But is HDXMS useful for detecting minute details in protein structure upon binding to an interaction partner? Our most recent work on Fox transcription factors is a fitting example of this phenomenon.

The Fox family of transcription factors is critical for key cellular processes such as cell growth, proliferation and longevity [30]. All members of the Fox family are characterized by having a highly-conserved DNA-binding domain of ~100 residues (namely, the forkhead domain) [31] and have been described as monomers in solution. However, *in vitro* evidence showed that the forkhead domain from members of the P subfamily (FoxP), which are highly critical in embryonic development due to their wide expression in the central nervous (FoxP1, FoxP2, and FoxP4), respiratory (FoxP1), and immune (FoxP3) systems [32], form dimers via three-dimensional domain swapping [33–35]. This process occurs when two or more monomers exchange identical regions or domains of their structure, reaching an intertwined quaternary assembly that is structurally identical to the monomeric state apart from the hinge region connecting the exchanged elements in the dimer [36]. To reach this oligomeric structure, intramolecular interactions between the exchanging elements and the rest of the protein are broken and then replaced in an intermolecular fashion [37]; thus, necessary local or even global unfolding must occur. Whilst for several years domain swapping was considered a structural vestige on the evolution of proteins towards oligomerization [38], several experiments have highlighted its functional relevance *in vivo*

Author Manuscript Author Manuscript Author Manuscript Author Manuscript

for FoxP3 [39] and the yeast homologous Fkh1 and Fkh2 [40] in allowing communication between distal chromosomal segments.

Recently, we explored the equilibrium folding landscape of the DNA-binding domain of FoxP1 under the presence of chaotropic agents as perturbants and using a combination of biophysical techniques, including circular dichroism, size exclusion chromatography and HDXMS [41]. For comparison, a monomeric mutant was constructed through a single-point mutation of an alanine in the hinge region, which is unique to the P subfamily of Fox transcription factors, to a proline that is highly conserved in all other subfamilies [35]. Our results revealed that the equilibrium unfolding of the monomeric mutant of FoxP1 A39P was best explained by a two-state N↔U folding mechanism between the native (N) and unfolded (U) states. In contrast, the unfolding of the wild-type dimer, whose dissociation constant ranged from 2 to 27 μM between 17 – 37 °C, was best explained by a three-state N2↔2I↔2U folding mechanism with a monomeric intermediate (I) with scarce loss of secondary structure (~15%). Moreover, size exclusion chromatography experiments in the presence of concentrations of denaturant in which the intermediate state is predominant showed that this state had ~20% higher hydrodynamic radius than the compact monomer. These data suggested that formation of the domain-swapped dimer of FoxP1 occurred through an intermediate, native-like state, rather than by following the complete unfolding/refolding mechanism that is canon for several protein models of domain swapping [42].

But what does the structure of the intermediate state “look” like when compared to the native state? To solve this, we again used HDXMS since it can easily handle the presence of chaotropic agents and other chemicals at high concentrations in the sample and during incubation in D_2O. While the presence of denaturant can potentially reduce proteolytic cleavage of the protein sample due to unfolding of pepsin, its concentration can be reduced during quenching of the exchange reaction, a step that precedes protease treatment and mass spectrometry analysis. We thus compared the local structural features of the wild-type FoxP1 monomer under native conditions and under conditions that favor the intermediate state, i.e. in the presence of 2 M guanidine hydrochloride, after 5 minutes of incubation in deuterated buffer, along with HDXMS measurements of the A39P mutant in the presence of the same concentrations of chaotropic agent [41].

This experiment allowed the comparison of peptides covering 84% of the total primary sequence of the forkhead domain of FoxP1. Hydrogen-deuterium exchange of the wild-type monomeric forkhead domain of FoxP1 unambiguously captured its native state, as demonstrated by the 0.81 correlation coefficient between the extent of exchange of all analyzed peptides and the solvent-accessible surface area (SASA) [42] calculated based on the solved NMR structure of the forkhead domain of FoxP1 (PDB ID 2KIU [35]). The native state exhibited an average deuterium exchange of 38%, whereas the intermediate state showed an average increase of 8% when compared to the native state. In contrast, the A39P mutant showed no significant differences when compared to the native wild-type monomer. Peptides with largest increases in deuterium exchange in comparison to the native monomer were located on secondary structure elements within the vicinity of helix H2 that serves as hinge region for the domain swapping of FoxP1 (Figure 2). These regions corresponded to strands S1 (17% increase in deuterium exchange), S2 and S3 (9% increase in deuterium

Author Manuscript Author Manuscript Author Manuscript Author Manuscript

exchange), which form a β-sheet within the same polypeptide chain only in the monomeric state but must break their interactions to enable domain swapping. Altogether, these results suggested that the intermediate state observed in our equilibrium folding experiments corresponded to an open native-like conformation in which strands S1-S3 became loose to allow domain swapping to occur, rather by needing complete protein unfolding to reach the native dimer form.

2.1.4 IκBα folds on binding to NFκB—IκBα is an inhibitor protein comprised of six ankyrin repeats that stack upon one another in a bent cylindrical structure upon interaction with the transcription factor NFκB. In 1998, two groups published structures of the NFκB(RelA-p50)-IκBα complex [43, 44]. Although only five ankyrin repeats (ARs) were predicted by sequence similarity, both structures showed six ankyrin repeats interacting by their β-hairpins with the dimerization domain interface of the NFκB molecule. HDXMS of IκBα free in solution revealed that the fifth and sixth ARs exchanged completely within one minute whereas the AR(1-4) segment exchanged much less, indicative of a folded structure [45]. Protein folding studies then revealed that only the AR(1-4) portion of the IκBα molecule constituted a cooperatively folding unit [46], but upon binding to NFκB all six ARs became folded as indicated by the dramatic decrease in amide exchange within AR(5-6) when IκBα was in complex with NFκB (Figure 3) [10]. Mutation of two residues in AR6 to the consensus residues for a stable AR resulted in much lower amide exchange in AR(5-6) in free IκBα and the inclusion of all six ARs in the cooperatively folding unit [47].

Although AR6 was predicted to be disordered, and exchanged all its amides, early studies had shown that no new helical structure was formed upon IκBα binding to NFκB. How, then, can we understand the structure of AR6? It couldn't be completely unfolded random coil, but it also couldn't be completely folded. Single molecule FRET studies in which donor and acceptor fluorophores were placed at AR2 and AR6 revealed that in physiological buffer and room temperature, the AR domain fluctuated stochastically between a high-FRET "folded" state which had the fluorophore distance expected from the crystal structure of the IκBα-NFκB complex to an ensemble of lower FRET states [48]. The mutant that had a stabilized AR6 did not fluctuate at room temperature, but began to fluctuate at 37°C. If the labels were placed at AR2 and AR5 in the wild type protein, fluctuations were not observed at room temperature, but were observed at 37°C [49]. These studies, along with flow-quench HDXMS [7] demonstrated that the AR(5-6) region of IκBα adopts an ensemble of folded and less-folded states which fluctuate over milliseconds-minutes.

Collaborative studies revealed that the weakly folded AR(5-6) has important regulatory function. In cells, free IκBα is degraded rapidly by a ubiquitin-independent process that was found to depend on the disorder of AR(5-6) [47]. A degron sequence was later found within AR6 that is responsible for ubiquitin-independent degradation of IκBα and when attached to other proteins, also causes them to be rapidly degraded [50]. It is possible to speculate that the proportion of degron-exposed states is tuned to define the degradation rate of free IκBα to exquisitely control its intracellular lifetime.

Author Manuscript Author Manuscript Author Manuscript Author Manuscript

2.2 Proteins that exhibit allosteric changes upon interaction with a binding partner

HDXMS can detect subtle changes in the native ensemble across the entire protein upon interaction with a ligand or another protein. To interpret these types of data, it is necessary to have at least one structure of the protein. Discovery of changes in protein dynamics upon binding is probably the most popular use of HDXMS today. Here we will highlight some of the early landmark studies in this area and then explore some recent studies from our own work.

The conformational changes associated with cAMP binding to the regulatory subunit of protein kinase A was shown to result in changes in the interface between the regulatory and catalytic subunits of the enzyme [51]. In this case, molecular docking results could be "filtered" by how well they matched the HDXMS data to produce a structure of the protein complex [52]. Larger structures of the kinase bound to A-kinase anchoring proteins were also explored [53]. Once the first structure of a protein kinase was solved in 1991[54], how the protein moved and whether it moved differently when the activation loop was phosphorylated could be revealed by HDXMS interpreted in light of the protein structure. The Ahn group's landmark study of the ERK kinases was first to reveal how activation loop phosphorylation altered kinase dynamics [55–57]. Engen and Smithgall used a combination of protein engineering and HDXMS to tease-apart the complex regulatory dynamics of the Src family of kinases [58–60].

HDXMS was also used to demonstrate that Taxol stabilizes microtubule dimers in a manner distinct from GDP or GTP. This system was really challenging because microtubules oligomerize and continuously hydrolyze GTP to GDP. By comparing microtubule samples bound to GDP or GTP or taxol, Horowitz's group was able to show that Taxol caused a marked reduction in deuterium incorporation in both β-and α-tubulin. When the regions of decreased deuterium incorporation were mapped onto the tubulin structure, new dimer-dimer interactions specifically induced by Taxol binding were revealed [61]. The results indicated that Taxol induced additional rigidity in addition to that caused by GTP-induced microtubule polymerization. The results showed how Taxol changes the tubulin conformation to act against microtubule depolymerization in a precise directional way [61]. Later, this same group was able to show how Taxol binding affects the binding of microtubule associated proteins [62].

Proteins involved in cell signaling often have several partners each of which specifies a particular functional task through allosteric modulation of the protein's structure and/or function [63]. We will present two recent examples of allosteric regulation, one from our own lab in which a transcription factor inhibitor kinetically controls DNA binding and the other from another lab in which substrate channeling was shown to control the degradation of the second messenger signaling molecule, cAMP.

2.2.1 Allostery within NFκB upon DNA or IκBα binding—The N-terminal DNA-binding domain (DBD) of p50 was removed for crystallization purposes, so only the RelA DBD was present [43, 44]. Because the RelA DBD was in a different location in the structure of IκBα-bound NFκB as compared to DNA-bound NFκB [64], it was suggested that IκBα altered the positions of the DBDs upon binding. Indeed, IκBα and DNA appeared

Author Manuscript Author Manuscript Author Manuscript Author Manuscript

to bind in a mutually-exclusive manner with IκBα winning the competition [65]. Using SPR and stopped-flow fluorescence, we showed that IκBα actually accelerates the dissociation rate of DNA from NFκB [66, 67]. Molecular Dynamics predictions based on an Associative Memory Hamiltonian energy function predicted that IκBα binding causes the NFκB DBDs to twist so that DNA can no longer bind [68]. Taking advantage of the Synapt G2Si with ion mobility, we were able to achieve over 90% sequence coverage of NFκB in the ~100kD NFκB-IκBα complex. Remarkably, IκBα binding to the dimerization domains caused reduced amide exchange throughout the DBDs as if it was causing them to be more well-folded [69]. Although the DBDs appear well-folded in the crystal structure, disorder prediction algorithms assign a high level of disorder to the RelA DBD and it is likely that the DBDs are more dynamic in solution than may be appreciated from the crystal structure in the presence of DNA. The long-distance folding of the NFκB DBDs must be attributed to allostery because the IκBα does not actually contact the DBDs at all! We see marked decreases in amide exchange throughout the DBDs when IκBα is bound whereas DNA binding causes both decreases and increases (Figure 4).

DNA binding to NFκB also elicited what appeared to be allosteric changes, this time resulting in increased amide exchange in loops within the dimerization domains, again far from the DNA binding site. A very interesting observation was that DNA binding caused dramatic increases in amide exchange in residues 300-320, which are predicted to be disordered, and which contain the nuclear localization sequence. The functional ramifications of this long-range increase in dynamics upon DNA binding are yet to be discovered.

These observations together with coarse-grained molecular simulations helped provide a mechanistic understanding of how IκBα facilitates the dissociation of NFκB from its transcription target sites [68]. Despite its large size, we were able to collect HDXMS data on the DNA-NFκB-IκBα transient ternary complex. The results showed that the IκBα had not fully achieved its folded and bound conformation in this intermediate state and its backbone fold adjusted to a less well-folded state throughout the last four ARs [70]. Thus, HDXMS experiments were able to aid in characterizing the intermediate ternary complex as IκBα engages the NFκB-DNA complex and folds while promoting dissociation of the DNA, a process we have termed molecular stripping.

2.2.2 Protein binding-induced allosteric effects and substrate channeling in the phosphodiesterase-protein kinase A complex—Often, cell signaling involves transient complex formation, which adds a layer of regulation that is critical for cell homeostasis [71]. The brief existence of transient complexes is crucial for cells to respond to highly dynamic changes in their immediate environment through coordinated responses in bacterial communities or cell tissues. Formation of these transient complexes enables the regulation through allosteric effects [63] and substrate channeling [72] between enzymes involved in the production and degradation of signaling molecules and other binding partners such as protein targets of these molecules.

This is the case for cyclic AMP (cAMP), an essential second messenger whose regulation as a signaling molecule is exerted in two phases. In the first phase, cAMP is synthesized by

Author Manuscript Author Manuscript Author Manuscript Author Manuscript

adenylyl cyclases after hormonal stimulation of G-protein coupled receptors. The cAMP then binds to specific targets such as protein kinase A (PKA), an important hub for several extracellular signals responsible for crucial cell regulation functions in almost all mammalian tissues [73]. In the second phase, cAMP signaling is terminated through cAMP hydrolysis to 5′-AMP by phosphodiesterases (PDEs), restoring basal intracellular concentration levels of this molecule facilitating a robust response to future stimuli [74]. Both the activation and termination phases of cAMP:PKA:PDE signaling are fabulous examples of ligand-induced allostery and substrate channeling that have been beautifully resolved through the use of HDXMS, as we will see next.

In its inactive state, PKA is an inactive tetrameric enzyme formed by two catalytic subunits (C) bound to a dimer of two regulatory subunits (R) that contains tandem arrays of two cyclic nucleotide-binding sites. Upon sequential binding of two cAMP molecules to domains B (which triggers conformational changes in domain A) and A for each R-subunit in the inactive PKA [75], dissociation between the R- and C-subunits and activation of the C-subunit to phosphorylate several protein targets is unleashed [51]. The A domain provides the primary interactions with the C-subunit as demonstrated by deletion mapping experiments [76]. Conversely, binding of the C-subunit to the cAMP-bound R-subunit leads to release of cAMP [77]. Insights into this mechanism of transient complex formation/dissociation was achieved through the use of HDXMS, which revealed the changes occurring in the R-subunit upon binding of cAMP and upon binding of the C-subunit [51]. To achieve this, HDXMS and careful analysis of 16 peptides covering 70% of the total sequence of a truncated form of the R-subunit RIα (residues 94-244), were made in the free, cAMP-bound and C-subunit bound states. The results demonstrated not only that helices A and B from the R-subunit were protected from deuterium exchange in 1-2 backbone amides upon binding of the C-subunit, thus participating in complex formation, but also that the phosphate-binding cassette where cAMP docks had increased amide exchange in the holoenzyme when compared to both the free and cAMP-bound states [51]. While tightening of the phosphate-binding cassette of domain A upon cAMP binding is expected, loosening of this region upon formation of the holoenzyme demonstrated that conformational changes were propagated to the cAMP-binding pocket of the R-subunit upon C-subunit binding. Further work with the full RIα protein led to demonstration that both cAMP binding sites in domains A and B exhibited increased amide deuterium exchange in the complex when compared to the free subunit, suggesting that these regions are primed to bind cAMP [78]. Conversely, cAMP binding led to increased amide exchange in the A domain that is the docking site for C-subunit [51]. Altogether, these results showed that mutually exclusive binding of either of these ligands to their corresponding binding sites transmitted long-range allosteric changes to the other binding site.

Given that the affinity of cAMP to the binding sites within the R-subunit is within the nanomolar range [79], an important question is how to release cAMP from its tight binding to PKA and successfully terminate cell signaling and to set-up a robust response to subsequent stimuli. Consequently, it was hypothesized that PDE can directly bind to the R-subunit of PKA to hydrolyze bound cAMP [80]. Therefore, an integrated strategy that combined HDXMS of the R-subunit RIα and PDE8A, fluorescence polarization assays, enzyme activity assays and computational docking was devised to demonstrate the formation

Author Manuscript Author Manuscript Author Manuscript Author Manuscript

of transient complexes that allowed communication between the cAMP binding sites of the R-subunit of PKA and PDE and substrate channeling [81, 82]. Fluorescence polarization assays on R-subunits labeled with a non-hydrolyzable cAMP analogue showed significant increases in fluorescence upon incubation with excess PDE8A, indicating dissociation of the cAMP analog from RIα. Having shown that PDE8A was capable of dissociating cAMP bound to RIα, HDXMS was performed on free PDE8A and on complexes formed between PDE8A and cAMP-free Riα. A total of 24 peptides that covered 72% of its catalytic domain were analyzed. Four regions showed decreased deuterium exchange upon binding to RIα, three of which are proximal to the catalytic site of PDE8A [81]. When mapping the changes in deuterium incorporation on the RIα subunit upon binding to the catalytic domain of PDE8A, it was revealed that both cAMP-binding sites from domains A and B of the R-subunit, the N-terminus and an interdomain helix showed decreased deuterium exchange, whereas the cAMP-bound RIα subunit only showed a decrease in deuterium exchange of larger magnitude in the nucleotide-binding sites.

Enzyme activity assays quantifying PDE-mediated cAMP hydrolysis showed unambiguously that the activity of PDE was enhanced 4- to 5-fold under the presence of RIα [82]. Therefore, a new set of experiments on a monomeric variant of RIα and the catalytic domain of PDE8A were setup, analyzing the differences in deuterium exchange between the free proteins, the binary complexes and the ternary complexes with bound cAMP. In this case, the PDE8A: RIα complexes exhibited a bimodal behavior in both nucleotide-binding sites of RIα during the exchange reaction up to 10 min followed by an increased unimodal exchange, whereas RIα only exhibited a unimodal behavior whose maximum extent of deuterium incorporation was similar to the less-exchanging population in the complex that lasted until 10 min of reaction. These results suggested that active association of RIα with PDE8A led to accumulation of a cAMP-free conformation. Similar experiments under excess cAMP revealed a substrate-dependent increase in the stability of the protein complex and allowed mapping of the interaction surfaces of both proteins, which mostly corresponded to loop regions in the vicinity of the two cyclic nucleotide binding sites of the R-subunit and the catalytic site of PDE8, such that a channel-like complex is formed that straddles the flexible cAMP binding sites where increased deuterium exchange due to cAMP hydrolysis is observed (Figure 5). These results, and the observation of a broadening of the mass envelopes as in a continuum between the cAMP-free and bound forms of RIα for peptides covering the nucleotide-binding sites of the R-subunit, strongly suggest substrate channeling between the binding sites of PDE8 and RIα [82].

2.2.3 Allostery in serine proteases revealed by HDXMS—One of the first demonstrations of the use of HDXMS to discover a protein-protein interface defined the thrombin-thrombomodulin interface between the 30s and 70s loops on the surface of thrombin [6]. The interaction between thrombin and thrombomodulin has an unusual thermodynamic signature; there is no favorable enthalpy change on binding, only a favorable entropy change. In contrast, a monoclonal antibody that competes with thrombomodulin for binding to thrombin shows a large favorable enthalpy change on binding [9]. In an effort to explain the unusual thermodynamic signature of thrombomodulin binding, a study of the pH-dependence of HDX at the interface was performed. The results, combined with

Author Manuscript Author Manuscript Author Manuscript Author Manuscript

computational analysis suggested that solvent expulsion from the interface could account for the entropic driving force for thrombin-thrombomodulin binding [8, 9].

With the advent of the Synapt G2Si, additional coverage of the thrombin sequence was obtained allowing discovery of the allosteric changes imparted to thrombin by binding of thrombomodulin. This study also revealed the dangers of interpreting serine protease function only from crystal structures, which must be inhibited or inactivated, and are sensitive to crystal packing forces. HDXMS of active thrombin in the absence of an inhibitor at its active site revealed high exchange of the critical N-terminus of the heavy chain. When serine proteases are proteolytically activated by cleavage between the light and heavy chains, the new N-terminus at the start of the heavy chain inserts into a pocket under the active site which is known to organize the catalytic triad [83]. This new N-terminus was never observed to be dynamic or to be anywhere but inside the pocket in any crystal structure, however, its amide exchange in active thrombin was higher than expected for a stably inserted N-terminus. Binding of an inhibitor at the thrombin active side resulted in markedly decreased amide exchange of the heavy chain N-terminus consistent with formation of the correct active site geometry. Interestingly, binding of thrombomodulin at the 30s and 70s loops on the back-side of thrombin also resulted in markedly decreased exchange of the heavy chain N-terminus as if thrombomodulin is allosterically activating thrombin catalysis [84].

Urokinase, a serine protease similar to thrombin, but involved in clot disruption, also was discovered by HDXMS to exist in a not-fully-active form when free in solution [85]. In this case, two crystal forms of urokinase were observed when the protein was crystallized in the absence of an active site inhibitor. One of the two β-barrels was completely disrupted in the “inactive” form and a β-strand that was supposed to be antiparallel had become parallel! HDXMS was used to prove that the inactive form actually existed in solution, apparently in equilibrium with the correctly-folded form. Although urokinase does not have a naturally-occurring allosteric regulator that binds at the 30s/70s loops, an inhibitory allosteric antibody was discovered that bound at this site. The urokinase in the antibody-urokinase structure appeared to adopt the “active” structure, but HDXMS revealed that in solution, the antibody completely converts urokinase to the “inactive” form (Figure 6) [85]. These results, in conjunction with activity assays and inhibitor-binding assays revealed the power of HDXMS to report on protein conformation in solution despite the misleading crystallographic results which apparently suffered from crystal packing forces. The fact that the antibody found the same allosteric site that thrombomodulin exploits suggests that the 30s/70s loop region may be an exploitable site for pharmaceutical attack on other medically-relevant serine proteases. In addition, an important conclusion from this work is that HDXMS results should at least qualitatively match crystallographic results, and when they don’t, it is likely that only one (perhaps minor) member of the solution structural ensemble may have been “trapped” in the crystal.

5. Conclusions

HDXMS has become a widely used approach for analyzing protein conformation. Although there are different schools of thought about how best to set-up the experiment, we have found that in general, analysis of the amides that exchange within 0-5 min under

Author Manuscript Author Manuscript Author Manuscript Author Manuscript

physiological temperature is most revealing for discovery of regions of disorder, regions that fold upon binding, and regions of the protein surface that become occluded from exchange upon interaction. With the advent of new instruments that enable orthogonal measurements on each peptide such as ion mobility, the resolution of thousands of peptides resulting from large complexes is now possible increasing the amount of the protein for which data can be obtained. The use of liquid handling robots has improved the reproducibility of the experiment so that even subtle differences in exchange caused by allosteric changes in protein dynamics can be confidently measured. While more labs are adopting HDXMS as a tool with which to probe protein dynamics, there still seems to be a lot to learn about the way proteins move and interact.

Supplementary Material

Refer to Web version on PubMed Central for supplementary material.

Acknowledgments

This work was supported by NIH grant P01GM071862 and R01 HL127041 to EAK, and FONDECYT 11140601 to CARS.

References

1. Dobson CM. Experimental investigation of protein folding and misfolding. Methods. 2004; 34:4–14. [PubMed: 15283911]
2. Eftink MR. The use of fluorescence methods to monitor unfolding transitions in proteins. Biophys J. 1994; 66(2 Pt 1):482–501. [PubMed: 8161701]
3. Royer CA. Probing protein folding and conformational transitions using fluorescence. Chem Rev. 2006; 106:1769–1784. [PubMed: 16683754]
4. Mulvihill MM, Guttman M, Komives EA. Protein interactions among Fe65, the low-density lipoprotein receptor-related protein, and the amyloid precursor protein. Biochemistry. 2011; 50(28): 6208–6216. [PubMed: 21650223]
5. Wand AJ, Roder H, Englander SW. Two-dimensional 1H NMR studies of cytochrome c: hydrogen exchange in the N-terminal helix. Biochemistry. 1986; 25(5):1107–1114. [PubMed: 3008820]
6. Mandell JG, Falick AM, Komives EA. Identification of Protein-Protein Interfaces by Decreased Amide Proton Solvent Accessibility. Proc Natl Acad Sci U S A. 1998; 95:14705–14710. [PubMed: 9843953]
7. Truhlar SM, Croy CH, Torpey JW, Koeppe JR, Komives EA. Solvent accessibility of protein surfaces by amide H/2H exchange MALDI-TOF mass spectrometry. J Am Soc Mass Spectrom. 2006; 17(11):1490–1497. [PubMed: 16934999]
8. Mandell JG, Baerga-Ortiz A, Akashi S, Takio K, Komives EA. Solvent accessibility of the thrombin-thrombomodulin interface. J Mol Biol. 2001; 306(3):575–589. [PubMed: 11178915]
9. Baerga-Ortiz A, Bergqvist S, Mandell JG, Komives EA. Two different proteins that compete for binding to thrombin have opposite kinetic and thermodynamic profiles. Protein Sci. 2004; 13(1): 166–176. [PubMed: 14691232]
10. Truhlar SM, Torpey JW, Komives EA. Regions of IkappaBalpha that are critical for its inhibition of NF-kappaB.DNA interaction fold upon binding to NF-kappaB. Proceedings of the National Academy of Sciences of the United States of America. 2006; 103(50):18951–6. [PubMed: 17148610]
11. Braselmann E, Chaney JL, Clark PL. Folding the proteome. Trends Biochem Sci. 2013; 38:337–344. [PubMed: 23764454]
12. Kuhner S, Van Noort V, Betts MJJ, Leo-Macias A, Batisse C, Rode M, Yamada T, Maier T, Bader S, Beltran-Alvarez P, Castano-Diez D, Chen WHWH, Devos D, Guell M, Norambuena T, Racke I,

Author Manuscript Author Manuscript Author Manuscript Author Manuscript

Rybin V, Schmidt A, Yus E, Aebersold R, Herrmann R, Bottcher B, Frangakis ASS, Russell RBB, Serrano L, Bork P, Gavin ACAC. Proteome Organization in a Genome-Reduced Bacterium. Science. 2009; 326:1235–1240. [PubMed: 19965468]

13. Gavin AC, Aloy P, Grandi P, Krause R, Boesche M, Marzioch M, Rau C, Jensen LJ, Bastuck S, Dümpelfeld B, Edelmann A, Heurtier MA, Hoffman V, Hoefert C, Klein K, Hudak M, Michon AM, Schelder M, Schirle M, Remor M, Rudi T, Hooper S, Bauer A, Bouwmeester T, Casari G, Drewes G, Neubauer G, Rick JM, Kuster B, Bork P, Russell RB, Superti-Furga G. Proteome survey reveals modularity of the yeast cell machinery. Nature. 2006; 440:631–636. [PubMed: 16429126]
14. Rumfeldt JAO, Galvagnion C, Vassall KA, Meiering EM. Conformational stability and folding mechanisms of dimeric proteins. Prog Biophys Mol Biol. 2008; 98:61–84. [PubMed: 18602415]
15. Balasubramaniam D, Komives EA. Hydrogen-exchange mass spectrometry for the study of intrinsic disorder in proteins. Biochem Biophys Acta. 2013; 1834:1202–1209. [PubMed: 23099262]
16. Ramírez-Sarmiento CA, Baez M, Wilson CAM, Babul J, Komives EA, Guixé V. Observation of solvent penetration during cold denaturation of E. coli phosphofructokinase-2. Biophys J. 2013; 104:2254–2263. [PubMed: 23708365]
17. Ramírez-Sarmiento CA, Baez M, Zamora RA, Balasubramaniam D, Babul J, Komives EA, Guixé V. The Folding Unit of Phosphofructokinase-2 as Defined by the Biophysical Properties of a Monomeric Mutant. Biophys J. 2015; 108:2350–2361. [PubMed: 25954892]
18. Gettins PG. Serpin structure, mechanism, and function. Chem Rev. 2002; 102:4751–4804. [PubMed: 12475206]
19. Gooptu B, Lomas DA. Conformational pathology of the serpins: themes, variations, and therapeutic strategies. Ann Rev Biochem. 2009; 78:147–176. [PubMed: 19245336]
20. Trelle MB, Madsen JB, Andreasen PA, Jørgensen TJ. Local transient unfolding of native state PAI-1 associated with serpin metastability. Angew Chem Int Ed Engl. 2014; 53(37):9751–9754. [PubMed: 25049220]
21. Petersen M, Madsen JB, Jørgensen TJD, Trelle MB. Conformational preludes to the latency transition in PAI-1 as determined by atomistic computer simulations and hydrogen/deuterium-exchange mass spectrometry. Sci Rep. 2017; 7(1):6636. [PubMed: 28747729]
22. Tsutsui Y, Liu L, Gershenson A, Wintrode PL. The conformational dynamics of a metastable serpin studied by hydrogen exchange and mass spectrometry. Biochemistry. 2006; 45(21):6561–6569. [PubMed: 16716066]
23. Tsutsui Y, Dela Cruz R, Wintrode PL. Folding mechanism of the metastable serpin α1-antitrypsin. Proc Nat Acad Sci USA. 2012; 109(12):4467–4472. [PubMed: 22392975]
24. Baez M, Wilson CAM, Ramírez-Sarmiento CA, Guixé V, Babul J. Expanded monomeric intermediate upon cold and heat unfolding of phosphofructokinase-2 from Escherichia coli. Biophys J. 2012; 103:2187–2194. [PubMed: 23200052]
25. Wetlaufer DB. Nucleation, Rapid Folding, and Globular Intrachain Regions in Proteins. Proc Nat Acad Sci USA. 1973; 70:697–701. [PubMed: 4351801]
26. Baez M, Wilson CAM, Babul J. Folding kinetic pathway of phosphofructokinase-2 from Escherichia coli: A homodimeric enzyme with a complex domain organization. FEBS Lett. 2011; 585:2158–2164. [PubMed: 21627967]
27. Shank EA, Cecconi C, Dill JW, Marqusee S, Bustamante C. The folding cooperativity of a protein is controlled by its chain topology. Nature. 2010; 465:637–640. [PubMed: 20495548]
28. Baez M, Babul J. Reversible unfolding of dimeric phosphofructokinase-2 from Escherichia coli reveals a dominant role of inter-subunit contacts for stability. FEBS Lett. 2009; 583:2054–2060. [PubMed: 19465020]
29. Cabrera R, Ambrosio ALB, Garratt RC, Guixé V, Babul J. Crystallographic Structure of Phosphofructokinase-2 from Escherichia coli in Complex with Two ATP Molecules. Implications for Substrate Inhibition. J Mol Biol. 2008; 383:588–602. [PubMed: 18762190]
30. Jackson BC, Carpenter C, Nebert DW, Vasiliou V. Update of human and mouse forkhead box (FOX) gene families. Hum Genomics. 2010; 4:345–352. [PubMed: 20650821]

Author Manuscript Author Manuscript Author Manuscript Author Manuscript

31. Clark KL, Halay ED, Lai E, Burley SK. Co-crystal structure of the HNF-3/fork head DNA-recognition motif resembles histone H5. Nature. 1993; 364:412–420. [PubMed: 8332212]
32. Tuteja G, Kaestner KH. SnapShot:Forkhead Transcription Factors I. Cell. 2007; 130(6):1160. [PubMed: 17889656]
33. Bandukwala HS, Wu Y, Feuerer M, Chen Y, Barboza B, Ghosh S, Stroud JC, Benoist C, Mathis D, Rao A, Chen L. Structure of a Domain-Swapped FOXP3 Dimer on DNA and Its Function in Regulatory T Cells. Immunity. 2011:479–491. [PubMed: 21458306]
34. Stroud JC, Wu Y, Bates DL, Han A, Nowick K, Paabo S, Tong H, Chen L. Structure of the forkhead domain of FOXP2 bound to DNA. Structure. 2006; 14:159–166. [PubMed: 16407075]
35. Chu YP, Chang CH, Shiu JH, Chang YT, Chen CY, Chuang WJ. Solution structure and backbone dynamics of the DNA-binding domain of FOXP1: Insight into its domain swapping and DNA binding. Protein Sci. 2011; 20:908–924. [PubMed: 21416545]
36. MacKinnon SS, Malevanets A, Wodak SJ. Intertwined Associations in Structures of Homooligomeric Proteins. Structure. 2013; 21:638–649. [PubMed: 23523426]
37. Yang S, Cho SS, Levy Y, Cheung MS, Levine H, Wolynes PG, Onuchic JN. Domain swapping is a consequence of minimal frustration. Proc Nat Acad Sci USA. 2004; 101:13786–13791. [PubMed: 15361578]
38. Nussinov R, Xu D, Tsai CJ. Mechanism and evolution of protein dimerization. Protein Sci. 1998; 7:533–544. [PubMed: 9541384]
39. Chen Y, Chen C, Zhang Z, Liu CC, Johnson ME, Espinoza C, Edsall LE, Ren B, Zhou XJ, Grant SF, Wells AD, Chen L. DNA binding by FOXP3 domain-swapped dimer suggests mechanisms of long-range chromosomal interactions. Nucleic Acids Res. 2015; 43:1268–1282. [PubMed: 25567984]
40. Ostrow AZ, Kalhor R, Gan Y, Villwock SK, Linke C, Barberis M, Chen L, Aparicio OM. Conserved forkhead dimerization motif controls DNA replication timing and spatial organization of chromosomes in S. cerevisiae. Proc Nat Acad Sci USA. 2017; 114:E2411–E2419. [PubMed: 28265091]
41. Medina E, Córdova C, Villalobos P, Reyes J, Komives EA, Ramírez-Sarmiento CA, Babul J. Three-Dimensional Domain Swapping Changes the Folding Mechanism of the Forkhead Domain of FoxP1. Biophys J. 2016; 110:2349–2360. [PubMed: 27276253]
42. Liu Z, Huang Y. Evidences for the unfolding mechanism of three-dimensional domain swapping. Protein Sci. 2013; 22:280–286. [PubMed: 23238853]
43. Huxford T, Huang DB, Malek S, Ghosh G. The crystal structure of the IkappaBalpha/NF-kappaB complex reveals mechanisms of NF-kappaB inactivation. Cell. 1998; 95(6):759–770. [PubMed: 9865694]
44. Jacobs MD, Harrison SC. Structure of an IkappaBalpha/NF-kappaB complex. Cell. 1998; 95(6): 749–758. [PubMed: 9865693]
45. Croy CH, Bergqvist S, Huxford T, Ghosh G, Komives EA. Biophysical characterization of the free IkappaBalpha ankyrin repeat domain in solution. Protein Sci. 2004; 13(7):1767–77. [PubMed: 15215520]
46. Ferreiro DU, Cervantes CF, Truhlar SM, Cho SS, Wolynes PG, Komives EA. Stabilizing IkappaBalpha by “consensus” design. Journal of molecular biology. 2007; 365(4):1201–16. [PubMed: 17174335]
47. Truhlar SME, Mathes E, Cervantes CF, Ghosh G, Komives EA. Pre-folding IkappaBalpha alters control of NF-kappaB signaling. J Mol Biol. 2008; 380:67–82. [PubMed: 18511071]
48. Lamboy JA, Kim H, Lee KS, Ha T, Komives EA. Visualization of the nanospring dynamics of the IkBa ankyrin repeat domain in real time. Proc Nat Acad Sci USA. 2011; 108:10178–83. [PubMed: 21628581]
49. Lamboy J, Kim H, Dembinski H, Ha TJ, Komives EA. Single molecule FRET reveals the native state dynamics of the IκBα ankyrin repeat domain. J Mol Biol. 2013; 425(14):2578–90. [PubMed: 23619335]
50. Fortmann KT, Lewis RD, Ngo KA, Fagerlund R, Hoffmann A. A Regulated, Ubiquitin-Independent Degron in IκBα. J Mol Biol. 2015; 427(17):2748–2756. [PubMed: 26191773]

Author Manuscript Author Manuscript Author Manuscript Author Manuscript

51. Anand GS, Hughes CA, Jones JM, Taylor SS, Komives EA. Amide H/2H exchange reveals communication between the cAMP and catalytic subunit-binding sites in the RIα subunit of protein kinase A. J Mol Biol. 2002; 323:377–386. [PubMed: 12381327]
52. Anand GS, Law D, Mandell JG, Snead AN, Tsigelny I, Taylor SS, Ten Eyck LF, Komives EA. Identification of the protein kinase A regulatory RIalpha-catalytic subunit interface by amide H/2H exchange and protein docking. Proc Nat Acad Sci USA. 2003; 100(23):13264–13269. [PubMed: 14583592]
53. Burns-Hamuro LL, Hamuro Y, Kim JS, Sigala P, Fayos R, Stranz DD, Jennings PA, Taylor SS, Woods VL. Distinct interaction modes of an AKAP bound to two regulatory subunit isoforms of protein kinase A revealed by amide hydrogen/deuterium exchange. Prot Sci. 2005; 14(12):2982–2992.
54. Knighton DR, Zheng JH, Ten Eyck LF, Ashford VA, Xuong NH, Taylor SS, Sowadski JM. Crystal structure of the catalytic subunit of cyclic adenosine monophosphate-dependent protein kinase. Science. 1991; 253:407–414. [PubMed: 1862342]
55. Resing KA, Ahn NG. Deuterium exchange mass spectrometry as a probe of protein kinase activation. Analysis of wild-type and constitutively active mutants of MAP kinase kinase-1. Biochemistry. 1998; 37(2):463–475. [PubMed: 9425067]
56. Hoofnagle AN, Resing KA, Goldsmith EJ, Ahn NG. Changes in protein conformational mobility upon activation of extracellular regulated protein kinase-2 as detected by hydrogen exchange. Proc Nat Acad Sci USA. 2001; 98(3):956–961. [PubMed: 11158577]
57. Dorey K, Engen JR, Kretzschmar J, Wilm M, Neubauer G, Schindler T, Superti-Furga G. Phosphorylation and structure-based functional studies reveal a positive and a negative role for the activation loop of the c-Abl tyrosine kinase. Oncogene. 2001; 20(56):8075–8084. [PubMed: 11781820]
58. Lerner EC, Trible RP, Schiavone AP, Hochrein JM, Engen JR, Smithgall TE. Activation of the Src family kinase Hck without SH3-linker release. J Biol Chem. 2005; 280(49):40832–40837. [PubMed: 16210316]
59. Hochrein JM, Lerner EC, Schiavone AP, Smithgall TE, Engen JR. An examination of dynamics crosstalk between SH2 and SH3 domains by hydrogen/deuterium exchange and mass spectrometry. Protein Sci. 2006; 15(1):65–73. [PubMed: 16322569]
60. Meyn MA, Wilson MB, Abdi FA, Fahey N, Schiavone AP, Wu J, Hochrein JM, Engen JR, Smithgall TE. Src family kinases phosphorylate the Bcr-Abl SH3-SH2 region and modulate Bcr-Abl transforming activity. J Biol Chem. 2006; 281(41):30907–30916. [PubMed: 16912036]
61. Xiao H, Verdier-Pinard P, Fernandez-Fuentes N, Burd B, Angeletti R, Fiser A, Horwitz SB, Orr GA. Insights into the mechanism of microtubule stabilization by Taxol. Proc Nat Acad Sci USA. 2006; 103(27):10166–10173. [PubMed: 16801540]
62. Xiao H, Wang H, Zhang X, Tu Z, Bulinski C, Khrapunovich-Baine M, Hogue Angeletti R, Horwitz SB. Structural evidence for cooperative microtubule stabilization by Taxol and the endogenous dynamics regulator MAP4. ACS Chem Biol. 2012; 7(4):744–52. [PubMed: 22270553]
63. Acuner-Ozbabacan SE, Engin HB, Gursoy A, Keskin O. Transient protein protein interactions. Protein Eng Des Sel. 2011; 24:635–648. [PubMed: 21676899]
64. Chen FE, Huang DB, Chen YQ, Ghosh G. Crystal structure of p50/p65 heterodimer of transcription factor NF-kappaB bound to DNA. Nature. 1998; 391(6665):410–3. [PubMed: 9450761]
65. Zabel U, Baeuerle PA. Purified human I kappa B can rapidly dissociate the complex of the NF-kappa B transcription factor with its cognate DNA. Cell. 1990; 61(2):255–65. [PubMed: 2184941]
66. Bergqvist S, Alverdi V, Mengel B, Hoffmann A, Ghosh G, Komives EA. Kinetic enhancement of NF-kappaB•DNA dissociation by IkappaBalpha. Proc Natl Acad Sci U S A. 2009; 106(46):19328–33. [PubMed: 19887633]
67. Alverdi V, Hetrick B, Joseph S, Komives EA. Direct observation of a transient ternary complex during IκBα-mediated dissociation of NF-κB from DNA. Proc Natl Acad Sci U S A. 2014; 111(1):225–230. [PubMed: 24367071]

Author Manuscript Author Manuscript Author Manuscript Author Manuscript

68. Potoyan DA, Zheng W, Komives EA, Wolynes PG. Molecular stripping in the NF-κB/IκB/DNA genetic regulatory network. Proc Natl Acad Sci U S A. 2016; 113(1):110–115. [PubMed: 26699500]
69. Ramsey KM, Dembinski HE, Chen W, Ricci CG, Komives EA. DNA and IκBα Both Induce Long-Range Conformational Changes in NFκB. J Mol Biol. 2017; 429(7):999–1008. [PubMed: 28249778]
70. Dembinski HE, Wismer K, Vargas J, Suryawanshi GW, Kern N, Kroon G, Dyson HJ, Hoffmann A, Komives EA. Functional consequences of stripping in NFkB signaling revealed by a stripping-impaired IkBa mutant. Proc Natl Acad Sci U S A. 2017 in press.
71. Nooren IMA, Thornton JM. Diversity of protein-protein interactions. EMBO J. 2003; 22:3486–3492. [PubMed: 12853464]
72. Ramírez-Sarmiento CA. "Riddle Me This": Substrate Channeling Solves the Paradigms of cAMP-Dependent Activation of PKA. Biophys J. 2017; 112:2451–2453. [PubMed: 28636902]
73. Taskén K, Aandahl EM. Localized effects of cAMP mediated by distinct routes of protein kinase A. Physiol Rev. 2004; 84:137–167. [PubMed: 14715913]
74. Skroblin P, Grossmann S, Schäfer G, Rosenthal W, Klussmann E. Mechanisms of Protein Kinase A Anchoring. Int Rev Cell Mol Biol. 2010; 283:235–330. [PubMed: 20801421]
75. Øgreid D, Døskeland SO. The kinetics of association of cyclic AMP to the two types of binding sites associated with protein kinase II from bovine myocardium. FEBS Lett. 1981; 129:287–292. [PubMed: 6269882]
76. Huang LJS, Taylor SS. Dissecting cAMP binding domain A in the R1α subunit of cAMP-dependent protein kinase: Distinct subsites for recognition of cAMP and the catalytic subunit. J Biol Chem. 1998; 273:26739–26746. [PubMed: 9756917]
77. Øgreid D, Døskeland SO. Cyclic Nucleotides Modulate the Release of [3H]Adenosine Cyclic 3′, 5′-Phosphate Bound to the Regulatory Moiety of Protein Kinase I by the Catalytic Subunit of the Kinase. Biochemistry. 1983; 22:1686–1696. [PubMed: 6303391]
78. Hamuro Y, Anand GS, Kim JS, Juliano C, Stranz DD, Taylor SS, Woods VL. Mapping intersubunit interactions of the regulatory subunit (RIα) in the type I holoenzyme of protein kinase A by amide hydrogen/deuterium exchange mass spectrometry (DXMS). J Mol Biol. 2004; 340:1185–1196. [PubMed: 15236976]
79. Herberg FW, Dostmann WRG, Zorn M, Davis SJ, Taylor SS. Crosstalk between Domains in the Regulatory Subunit of Camp-Dependent Protein-Kinase - Influence of Amino-Terminus on Camp Binding and Holoenzyme Formation. Biochemistry. 1994; 33:7485–7494. [PubMed: 8003514]
80. Moorthy BS, Gao Y, Anand GS. Phosphodiesterases Catalyze Hydrolysis of cAMP-bound to Regulatory Subunit of Protein Kinase A and Mediate Signal Termination. Mol Cell Proteomics. 2011; 10 M110.002295.
81. Krishnamurthy S, Moorthy BS, Xiang LX, Shan LX, Bharatham K, Tulsian NK, Mihalek I, Anand GS. Active site coupling in PDE:PKA complexes promotes resetting of mammalian cAMP signaling. Biophys J. 2014; 107:1426–1440. [PubMed: 25229150]
82. Tulsian NK, Krishnamurthy S, Anand GS. Channeling of cAMP in PDE-PKA Complexes Promotes Signal Adaptation. Biophys J. 2017; 112:2552–2566. [PubMed: 28636912]
83. Hedstrom L. Serine protease mechanism and specificity. Chem Rev. 2002; 102:4501–4524. [PubMed: 12475199]
84. Handley LD, Treuheit NA, Venkatesh VJ, Komives EA. Thrombomodulin Binding Selects the Catalytically Active Form of Thrombin. Biochemistry. 2015; 54(43):6650–6658. [PubMed: 26468766]
85. Kromann-Hansen T, Lange LE, PH S, Hassanzadeh-Ghassabeh G, Huang M, Jensen JK, Muyldermans S, Declerck PJ, Komives EA, Andreasen PA. Discovery of a novel conformational equilibrium in urokinase-type plasminogen activator. Sci Rep. 2017; 7(1):3385. [PubMed: 28611361]

Author Manuscript Author Manuscript Author Manuscript Author Manuscript

Highlights

- Use of a combination of biophysical techniques with amide hydrogen/deuterium exchange mass spectrometry (HDXMS) reveals mechanisms of folding upon binding
- HDXMS is an ideal method for discovering regions of proteins that change their “foldedness” upon interaction
- HDXMS reveals how changes in dynamics are propagated long distances through proteins and these allosteric effects reval important functional changes in catalytic activity and substrate channeling

Author Manuscript Author Manuscript Author Manuscript Author Manuscript

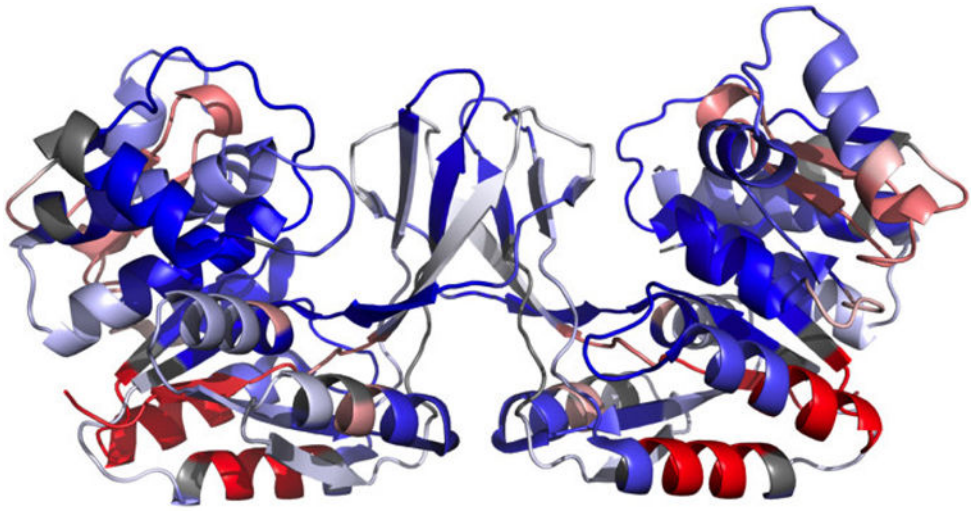

Figure 1.

Exchange difference between the native dimer of Pfk-2 and a monomeric mutant generated through a single-point mutation on the bimolecular domain that constitutes the protein-protein interface. Exchange is presented as a color gradient from blue to white to red, with blue meaning no difference in exchange between dimer and monomer, and red being 25% more exchange in the monomeric state. It is clear that one strand at the interface is more exposed in the mutant (white) whereas the other strand remains completely folded (blue). Also, regions of the large domain of the protein that are wired to the bimolecular domain through the connectivity of the chain topology exhibit more exchange in the monomeric state (helices in red). Residues with no counterpart between the wild type protein and the monomeric mutant are shown in gray.

Author Manuscript Author Manuscript Author Manuscript Author Manuscript

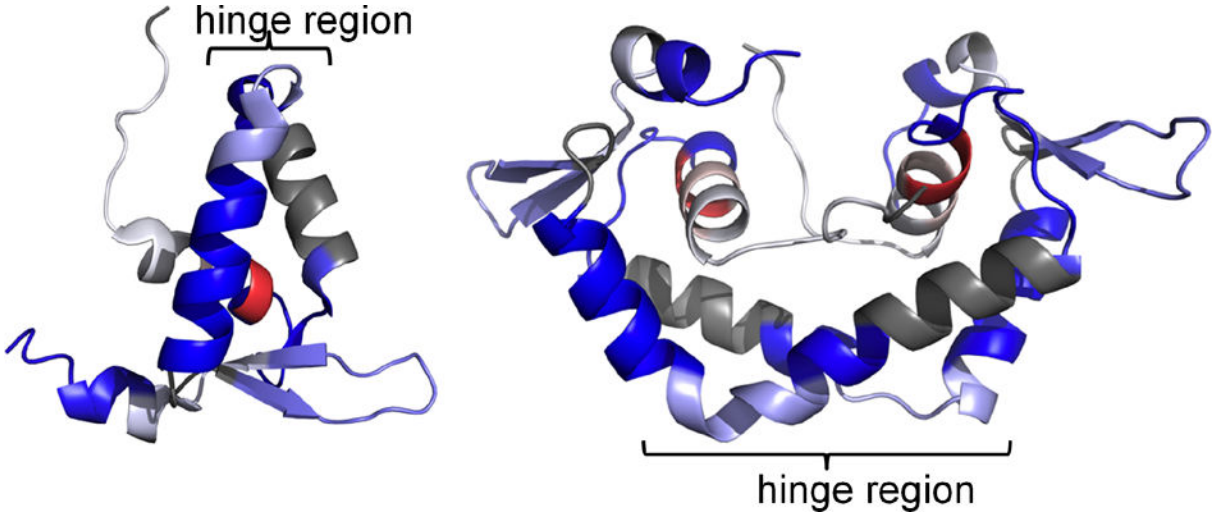

Figure 2.

Exchange difference between the native monomer of FoxP1 and the intermediate state populated at 2 M GndHCl, presented in the structure of the monomer (left) and the domain-swapped dimer (right). Exchange is presented as a color gradient from blue to white to red, with blue meaning no difference in exchange between dimer and monomer, and red being 25% more exchange in the intermediate state. The regions with more differences in exchange correspond to the hinge helix that enables domain swapping and in the strands that are packed together only in the monomeric state of FoxP1 (light blue and white), as well as the N-terminal helix (white and red). Residues not captured during mass spectrometry are shown in gray.

Author Manuscript Author Manuscript Author Manuscript Author Manuscript

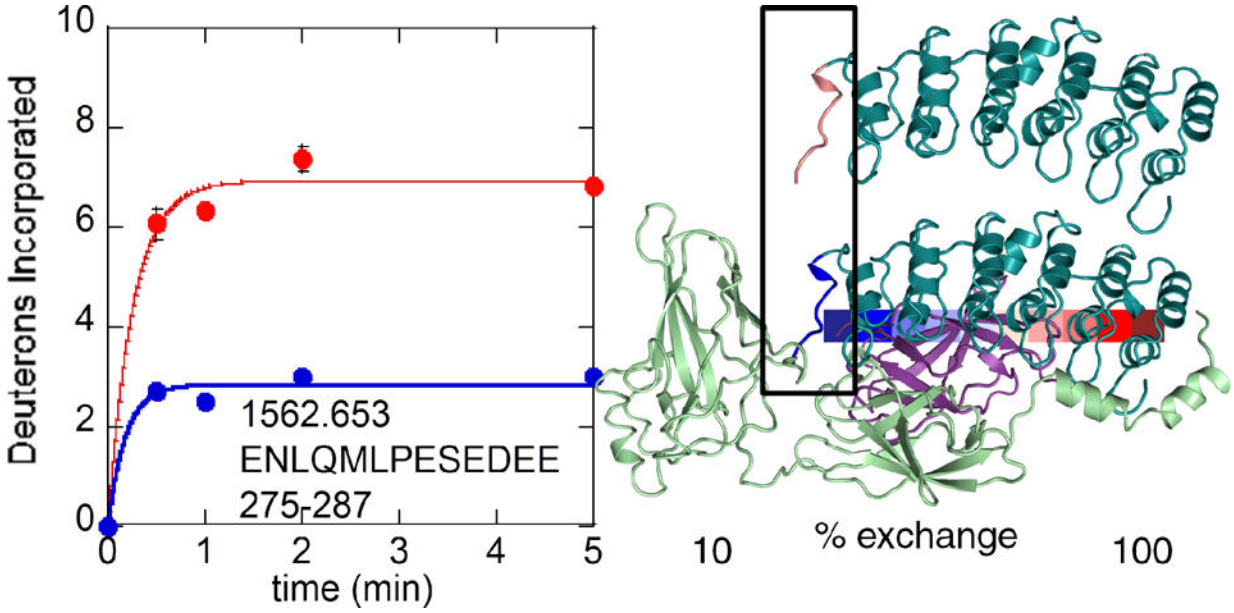

Figure 3.

Deuterium uptake in the very C-terminus of IκBα is dramatically reduced upon binding to NFκB. The plot of uptake for one peptide corresponding to residues 275-287 is shown for free IκBα (red circles) and in complex with NFκB (blue circles). This region of the protein is shown in the structures of the free protein (top) and the bound protein (bottom) with residues 275-287 colored according to their deuterium uptake.

Author Manuscript Author Manuscript Author Manuscript Author Manuscript

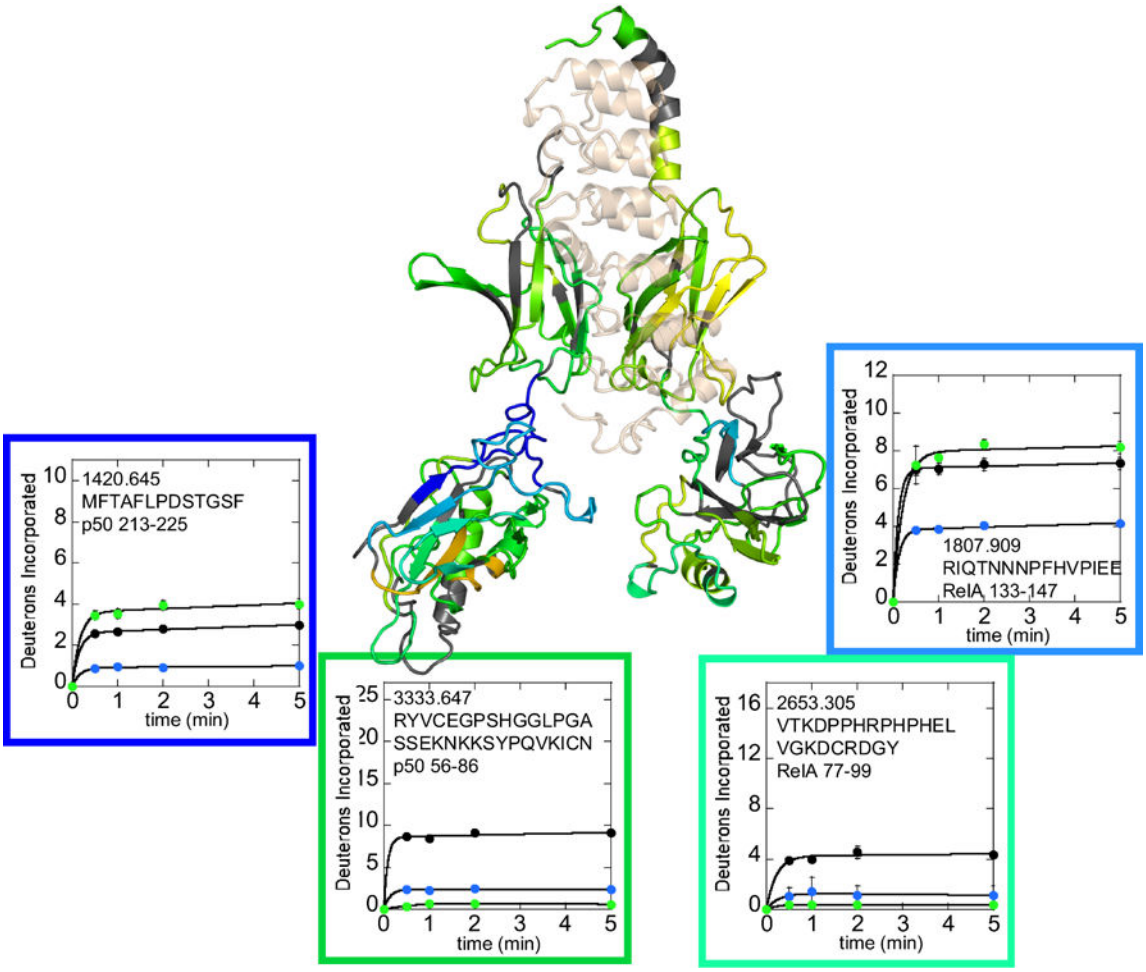

Figure 4.

A complete model of the structure of the NFκB-IκBα complex is shown with the NFκB RelA and p50 colored according to the difference in deuterium uptake between the free NFκB and the IκBα-bound NFκB. The difference is colored on a rainbow scale with blue being >50% decrease in exchange and red being >50% increase in exchange. The DBDs are not in contact with the IκBα (colored in wheat) and yet they exchange dramatically less in the IκBα bound form. Deuterium uptake plots for selected regions are also shown with free NFκB (black circles), IκBα-bound NFκB (blue circles) and DNA-bound NFκB (green circles). Two regions that show dramatic decreased in exchange upon IκBα binding show increases in exchange upon DNA binding.

Author Manuscript
Author Manuscript
Author Manuscript
Author Manuscript

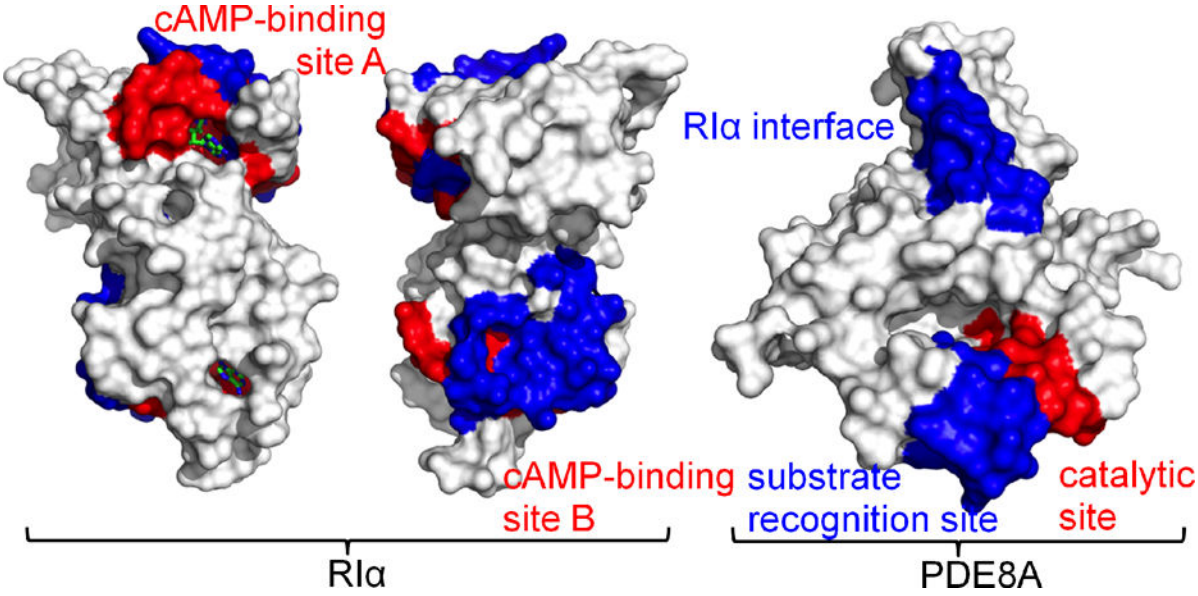

Figure 5.

Protein-protein interaction interfaces identified near the cAMP binding sites of RIα and PDE8A through HDXMS. The regions shown in blue for RIα (left) correspond to the cAMP interaction sites A and B with PDE8A, as evidenced by the decrease in deuterium exchange upon binding to PDE8A, whereas the regions in red are the sites at which an increase in deuterium exchange was observed. The regions shown in blue for PDE8A (right) correspond to the protein interaction interface and the substrate recognition site where decreased hydrogen deuterium exchange was observed upon binding to RIα, whereas the region in red corresponds to the catalytic site of PDE8A where increased deuterium exchange was observed. These results suggest the formation of a channel-like complex between the binding sites of both proteins and an allosteric mechanism by which which cAMP is channeled from RIα to PDE8A.

Author Manuscript Author Manuscript Author Manuscript Author Manuscript

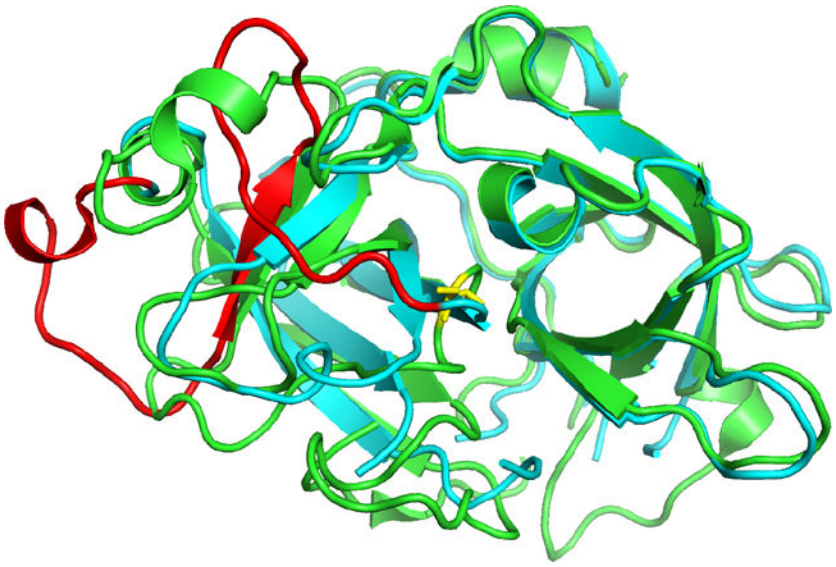

Figure 6.

Structures of urokinase from the crystal structure (PDB 5LHS) showing the region that is disordered upon binding of the inhibitory antibody in red. This region shows dramatic increases in exchange upon antibody binding as compared to the protein without antibody bound (green).